Noname manuscript No.
(will be inserted by the editor)

Evaluation of a geometry-based knee joint compared to a planar knee joint

Anders Sandholm[1] · **Cédric Schwartz**[2] · **Nicolas Pronost**[1,3] · **Mark de Zee**[2] · **Michael Voigt**[2] · **Daniel Thalmann**[1]

Abstract Today neuromuscular simulations are used in several fields, such as diagnostics and planing of surgery, to get a deeper understanding of the musculoskeletal system. During the last year new models and datasets have been presented which can provide us with more in-depth simulations and results. The same kind of development has occurred in the field of studying the human knee joint using complex three dimensional finite element models and simulations. In the field of musculoskeletal simulations, no such knee joints can be used. Instead the most common knee joint description is an idealized knee joint with limited accuracy or a planar knee joint which only describes the knee motion in a plan. In this paper, a new knee joint based on both equations and geometry is introduced and compared to a common clinical planar knee joint. The two kinematical models are analyzed using a gait motion, and are evaluated using the muscle activation and joint reaction forces which are compared to in-vivo measured forces. We show that we are able to predict the lateral, anterior and longitudinal moments, and that we are able to prediction better knee and hip joint reaction forces.

Keywords Knee joint · Inverse kinematics and dynamics · Joint reaction · Computed Muscular Control · OrthoLoad · Validation · Musculoskeletal model

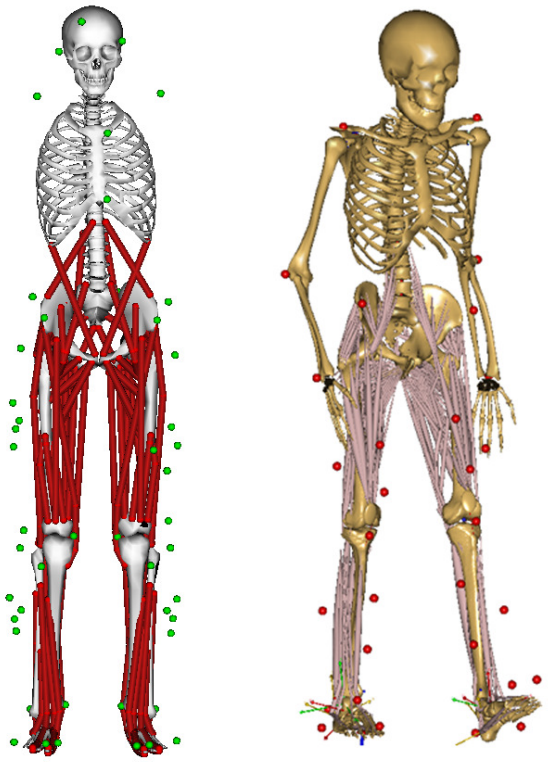

Fig. 1 Left: OpenSim model with planar knee joint scaled into subject, Right: Anybody model with the geometry knee joint.

1 Introduction

Today the field of neuromuscular simulations is widely used to understand the underlying dynamics of the movement of living beings, from gait research, treatment of patient with gait problems, to the teaching of physicians and the development of ergonomic furniture. During the last few years several platforms have been developed from commercial tools [7] to open-source based solutions [8]. The expansion of this field has also allowed the accessibility to musculoskeletal models that are able to describe different levels of complexity [9,32,4]. This development has given researchers and physicians powerful tools to analyze advanced simulations and even to execute 'what-if' scenarios before clinical treatment has even started. A problem with most of these models is that the human knee joint description is still rather undeveloped. This comes from the underlying complexity of the knee. Where as the hip joint can be described during normal gait as a standard ball-socket joint with no translations and the ankle-subtalar joint as two revolute joints. The knee joint motion is much more com-

[1] École Polytechnique Fédérale de Lausanne - Virtual Realtiy Lab (Lausanne, Switzerland)
[2] Aalborg University - Center for Sensory-Motor Interaction - (Aalborg, Denmark)
[3] Utrecht University - Games and Virtual Worlds (Utrecht - The Netherlands)

plexed including both translations and rotations during normal gait motions. In daily activity, such as normal non-pathological gait, the human knee joint is subjected to significant loads with peak values well-above the subject's body weight [3,10,13,15,21]. These load patterns are very complex, because of several external forces exist (ground reaction force, mass and acceleration forces from the foot and the shank) which are counterbalanced by the forces acting inside the joint, such as the tibiofemoral contact forces and forces generated by the muscles to either keep the balance or to generate a motion. There are also smaller forces acting inside the joint such as soft tissue constraints, contact forces and forces created by internal friction. Due to this complexity the knee joint has mostly been modeled and simulated using finite element method (FEM), which has been used in great success to analyze joint kinematics and a variety of problems relating to the knee joint [24,11,12]. In these models the knee includes structures as ligaments and sophisticated materials [31,23] which implement properties as transverse isotopy, nonlinear stress-strain curve and to a certain degree viscoelastic behavior. In musculoskeletal models joints are not described as three dimensional meshes that are allowed to deform, instead joint kinematics are modeled as one or several functions controlled by one or several variables. This has led to the fact that in most common musculoskeletal models the human knee joint is either described as an idealized joint based only on rotations [16] or, as in most common clinical models, a planer knee joint [9]. In *Delp et al., 1990* the knee joint is described using one degree of freedom (DoF) (knee flexion), with an additional two coupled DoFs, tibiofemoral translation and the nonsagittal rotation. A recent new knee model [4] was published which uses one DoF (flexion) but with additional coupled dimensions to incorporate three translations and rotations of the tibia relative to the femur. This knee joint is based on tibiofemoral kinematics experimental measurements from 23 'normial-sized' adult knees [30, 20]. In this paper a new knee joint is presented which combines the geometric description from a finite element method and the functional description of musculoskeletal joints. The joint is based on the work of *Walker et al., 1988* [30] and *Kurosawa et al., 1985* [20]. The knee joint is defined as three DoFs, driven by flexion, with additional adduction-abduction rotation and distration-compression translation described from the subject's knee geometry/anatomy.

2 Material and Methods

In this study a 34 year old male, weighing of 89.6 kg with no recorded knee injury or other muscular or skeletal injuries were studied. Initially a MRI acquisition (resolution: 0.39 x 0.39 x 1mm) of the subject's knee was performed. Both lateral and femoral knee condyles were segmented including cartilage (see fig. 2(a)) [26, 27]. Gait motions were captured using eight cameras (Qualisys ProReflex, 200 Hz) and two AMTI force platforms (2000 Hz). During the motion capture eight electromyography sensors were used to record muscle activation in biceps femoris long head (BFLH), gastronemius (GAS), glutes maximus (GMAX), rectus femoris (RF), soleus (SOL), tibalius anterior (TA), vastus lateralis (VL) and vastus medialis (VM). During the motion capture the Cleveland Clinic marker set was used [6], with additional four marker plates (each containing four reflective markers) placed on the lateral side of each thigh and shank. Kinematic and kinetic data along with EMG was extracted from C3D files using the MotionLab Matlab toolbox [25] and filtered using a third order kalman filter [19] to ensure accurate an inverse kinematic solution [14]. The same data was exported to OpenSim and AnyBody formats. The subject kept a constant speed of 1.86m/s during the gait motion.

2.1 Geometry-based knee joint

To develop the geometry-based knee joint the AnyBody Modeling System [7] was used.The geometry-based knee joint is defined to use knee flexion-extension from the subject's gait motion as the driving DoF. The other five DoF are defined depending on the position of the joint, adduction-abduction rotation and distration-compression translation were constrained using the subject's knee anatomy, two (posterior-anterior translation and internal-external rotation) were driven by equations from *Walker et al., 1988* [30] and *Kurosawa et al., 1985* [20], the medial-lateral translation was locked.

The construction of these constraints was achived using three main steps:

1. Extraction of anatomical information
2. Information registration in the biomechanical model
3. Contact definition between the tibia and the femur

In the first step a quadric robust-fitting approach [2] was used to model the condyles. The fitting methods resulted in two ellipsoids, one for each condyle (see fig. 2(b)). The lateral and medial plateaus were described as two contact points which were determined as the closest points between the femoral and tibial prosthesis components. The second step involved the registration of the anatomical information in AnyBody: the knee model is based on the patient's anatomy represented as the ellipsoids and the contact points which

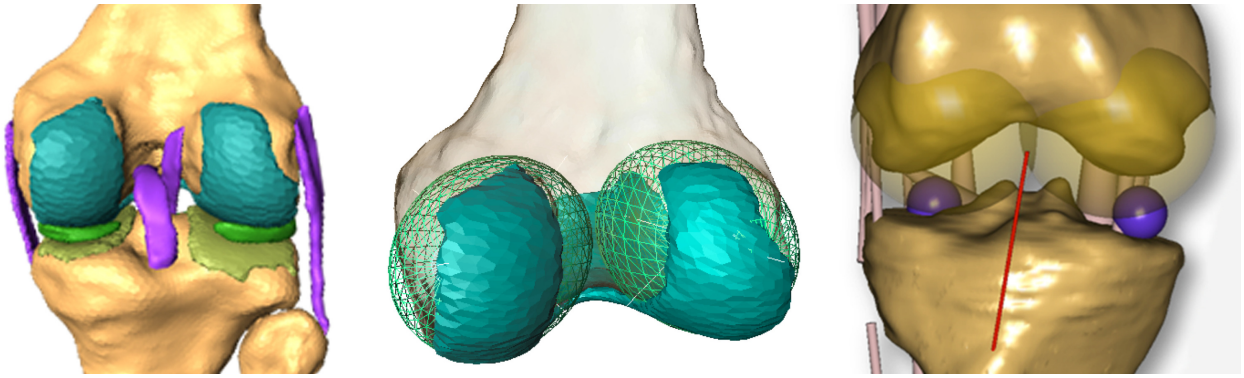

(a) Segmentation result of the knee joint including cartilage and menisci.

(b) Condyles with each registered ellipsoid

(c) Complete knee joint visualization. Contact points shown as violet spheres. The ellipsoids do not here aligned up with the femur because AnyBody visualize the femur with an generic model, not the subject specific femur used in the modelization.

Fig. 2 Stages of modeling the geometry knee joint

were described in an AnyBody biomechanical model. The thigh segment (ellipsoids) registration was produced using the hip center and the two femoral epicondyles (see fig. 3). The shank segment (contact points) registration was realized using the two ankle malleolars and the tibia tuberosity. In the third step a model constraint was introduced to ensure contact between the lateral and medial ellipsoids and two points located respectively on the lateral tibial plateau and the medial tibial plateau (see fig. 2(c)). To model the displacement that occurs in the knee during gait, [1], the geometry-based knee joint also includes posterior-anterior translation and internal-external rotation given by the equations provided in *Walker et al., 1988* [30]. Only the linear term was modeled and applied to the contact points relativel to the tibia segment.

Fig. 3 Localization of the three landmarks used for the registration of the femur in the biomechanical model (yellow spheres) medial and lateral epicondyles as well as the center of the femoral head, which was obtained after fitting a sphere (green mesh) on the articular surface of the femoral head.

2.2 Planar knee joint

The second knee model that we used in this study is the *Yamaguchi et al 1989* [32], which is described as a planar knee joint which works in a plane using one DoF . The motion of the knee joint is represented by a pathway for the center of rotation that gives realistic orientations of the femur relative to the tibia. The joint uses two additional coupled DoF (posterior-anterior and distration-compression), described as functions of one rotational degree of freedom (knee flexion). These two relationships give the rolling-to-sliding ratio of the motion of the femoral condyles on the tibial plateau.

2.3 A common model

In order to evaluate the geometry-based knee joint and to compare result to the planar knee joint a common neuromuscular model and simulation platform must be used. Therefore a common model [9] was agreed upon consisting of a torso (including head) modeled as a ridged element with three rotational DoF relative to the pelvis. The pelvis could rotate and translate in all three dimensions. The hip joint was modeled as a ball-socket joint with three rotation DoF. The ankle-subtalar complex was represented by two revolute joints aligned with anatomical axes. The metarsophalangeal joint was modeled as a one DoF hinge joint which allowed flexion and extension. In both systems the model was scaled to a subject-specific geometry that was based on the markers' position during a static trial which was followed by an inverse kinematic trial where joint

angles and translations were determined. Both models were consistent as regarding body elements and marker weights. Only the right knee joint was different. To be able to express the geometry-based knee joint kinematic in OpenSim, a new model, was created using a free six DoF knee joint. To translate the geometry-based knee joint kinematic to the new OpenSim model a common coordinate system was created for each body part using motion capture markers. Using these common coordinate systems for each frame of kinematic solution, a translation and rotation matrix was calculated which translated the femur and tibia kinematics from the Anybody system into OpenSim coordinate system. The neuromuscular models used to estimate muscle forces consisted of 92 muscle actuators [8].

2.4 Dynamic simulation

To investigate both knee joints and their ability to predict forces OpenSim 2.0 was used. First, inverse dynamics were used to study the generalized forces acting upon each joint. Second, computed muscular control (CMC) [29] was used to find the optimal muscle excitation pattern that would drive the models along the desired trajectories. Third, a joint reaction analyze was carried out that calculate forces and moments acting on the hip and knee joint using the muscle forces estimated during CMC. During the simulations both models used the same marker weight/cost functions and optimization values. The result from all three simulations were extracted using MotionLab and normalized over the gait cycled. EMG signals were extracted, normalized to the gait cycle then high pass filtered (20 Hz), rectified and finally low pass filtered (6 Hz).

3 Result

To evaluate the geometry knee joint result will be compared to the common used planar knee description. Result from inverse dynamics, computed muscular controls and joint reactions from both the hip joint and knee joint will be presented using both knee joint models.

3.1 Inverse Dynamics

Inverse Dynamic is a common way to investigate the generalized forces that acts upon joints given a specific motion. This is done by using information from the model such as body mass, inertia and kinematics (acceleration) to solve the second fundamental law of motion.

In figure 4(a) hip joint flexion moment is shown. The literature data have been normalized to the subject's body weight and leg length and shown in newton meters (Nm). Both knee joints show similar result with the data published by *Kadaba et al., 1989* [18]. The planar knee joint model predict a hip flexion moment that has a mean of 12 Nm larger than the value predicted by the geometry-based knee joint model. Hip adduction moment (fig. 4(b)) correspond also with the data published by *Kadaba et al., 1989*. The planar knee joint model produce a mean value which is 8 Nm higher then the geometry-based knee joint model. Figure 4(c)) shows hip rotation moment, both the geometry-based knee joint model and the planar knee joint model show resemblance with the data published by *Kadaba et al., 1989*. The planar knee joint model estimate a moment larger by a mean of 2.2 Nm compare to the geometry-based knee joint model. Both knee joints display an oscillation starting at around 60% of the gait cycle and continue during the swing phase. This comes from the subject's foot motion during toe off and swig phase.

Inverse dynamics results for knee flexion are shown in figure 4(a). Here clear differences between the geometry-based knee joint and the planar knee joint model are present. The geometry-based knee joint display the same trend as data published by *Kadaba et al., 1989*. While during the stance phase the planar knee join correspond to data published by *Cappozzo et al., 1975* and during the swing phase it correspond to data published by *Patriarco et al. 1981*. The mean difference between the planar knee joint and the geometry-based knee joint are 58 Nm. The largest contribution to the mean difference comes from the two trends shown during the stance phase. The planar knee joint model reaches its maximum value at 22% of the gait cycle while the geometry-based knee joint reaches its maximum value first at 40% of the gait cycle. Figure 5(b) show moment forces for adduction and rotation. These dimensions are not present in the planar knee joint and therefore no moment are calculated for them. Neither have any literature data been published for knee adduction/rotation moment forces.

3.2 Muscle estimation

Computed muscular control activation pattern from both knee models (fig. 6) were in general consistent with the captured EMG pattern, although there are clear differences between the two knee joint models. In fig. 6 the grey area represents ± 1 standard deviation of the EMG signal calculated from 28 gait motions, which were all acquired during the same motion capture session.

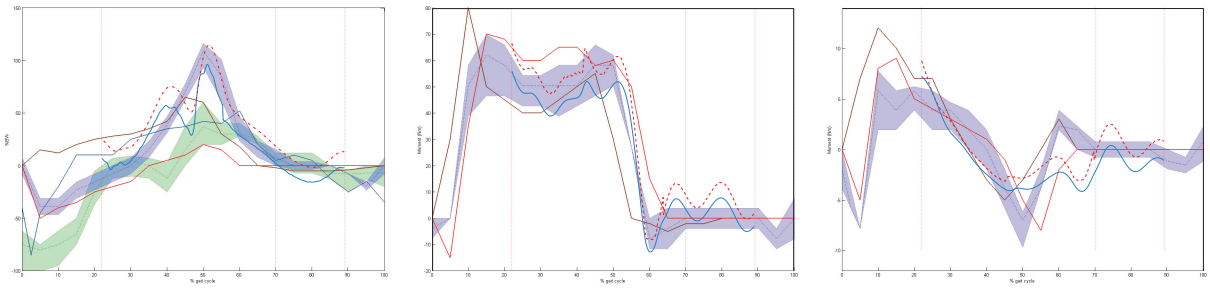

(a) Flexion (b) Adduction (c) Rotation

Fig. 4 Moment working on the hip joint from inverse dynamics. Blue solid line moment from geometry knee joint, red dashed line moment from planar knee joint, *Cappozzo et al., 1975* = Green area, mean value dotted green line; *Patriarco et al. 1981* = brown line; *Cowninshield et al., 1978* = red solid line; *Kadaba et al., 1989* = blue area, mean = dotted line; *Inman et al., 1947* = dark blue line

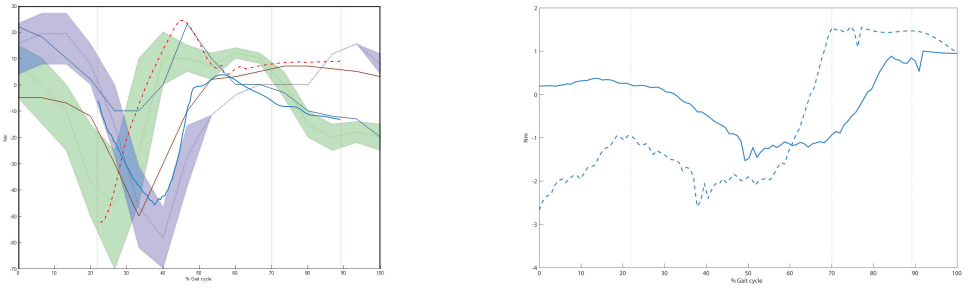

(a) Knee Flextion (b) Knee Adduction and Rotation

Fig. 5 (a); Moment working on the hip joint from inverse dynamics. Blue solid line moment from geometry knee joint, red dashed line moment from planar knee joint, *Cappozzo et al., 1975* = Green area, mean value dotted green line; *Patriarco et al. 1981* = brown line; *Kadaba et al., 1989* = blue area, mean = dotted line; *Inman et al., 1947* = dark blue line. (b); Solid line = knee rotation, dashed = knee adduction.

For the hip extender/abductor GMAX (fig. 6(c)) a small differences in activation pattern exist, the planar knee joint model predict a slightly higher activation value then the geometry-based knee joint. For VM (fig. 6(h)) which is a knee extender two patterns are present. First the geometry-based knee joint model display a better prediction of activation during the stance phase. Second, the planar knee joint model predict an activation in VM starting at 80% of the gait cycle, this muscle activation is not present in the geometry-based knee joint model. The second knee joint extender VL (fig. 6(g)) display a large difference between the two knee joint models. The planar knee joint model predicts no activation for VL during the mid-stance phase, which the geometry-based knee joint model predicts. The planar knee joint model also show an activation before toe-off in VL, which also is slightly present in the geometry-based knee joint. For the muscles spanning over the ankle joint some difference exist between the two models. SOL (fig. 6(e)) show a similar activation pattern for the two knee joint models. For TA (fig. 6(f)) the models predict different activation during the stance-phase. The EMG pattern for TA show a large activation during heel-strike which is deactivated around 10-15 % of the gait cycle. In the planar knee joint model this activation is still present until 34% of the gait cycle. The geometry-based knee joint model show no activation from 22% of the gait cycle were the CMC simulation start in this study. For the muscle spanning both the hip joint and the knee joint ,BFLH (fig. 6(a)) and RF (fig. 6(d)), similar differences are seen in the patterns between the two knee models. The geometry-based knee joint model predicted a lower activation during the toe off then the planar knee joint model. The planar knee joint model predicts a higher activation of the RF after toe off, which is not present in the captured EMG. For the muscle GAS (fig. 6(b)) which spans over both the knee joint and the ankle joint a clear difference between the models are present. The planar knee joint model predict a mean of 24% higher activation until 50% in the gait cycle and then 10% higher activation until 60% in the gait cycle. From 60% and during toe-off the planar knee joint model predict a higher activation with a mean of 12% than the geometry-based knee joint model.

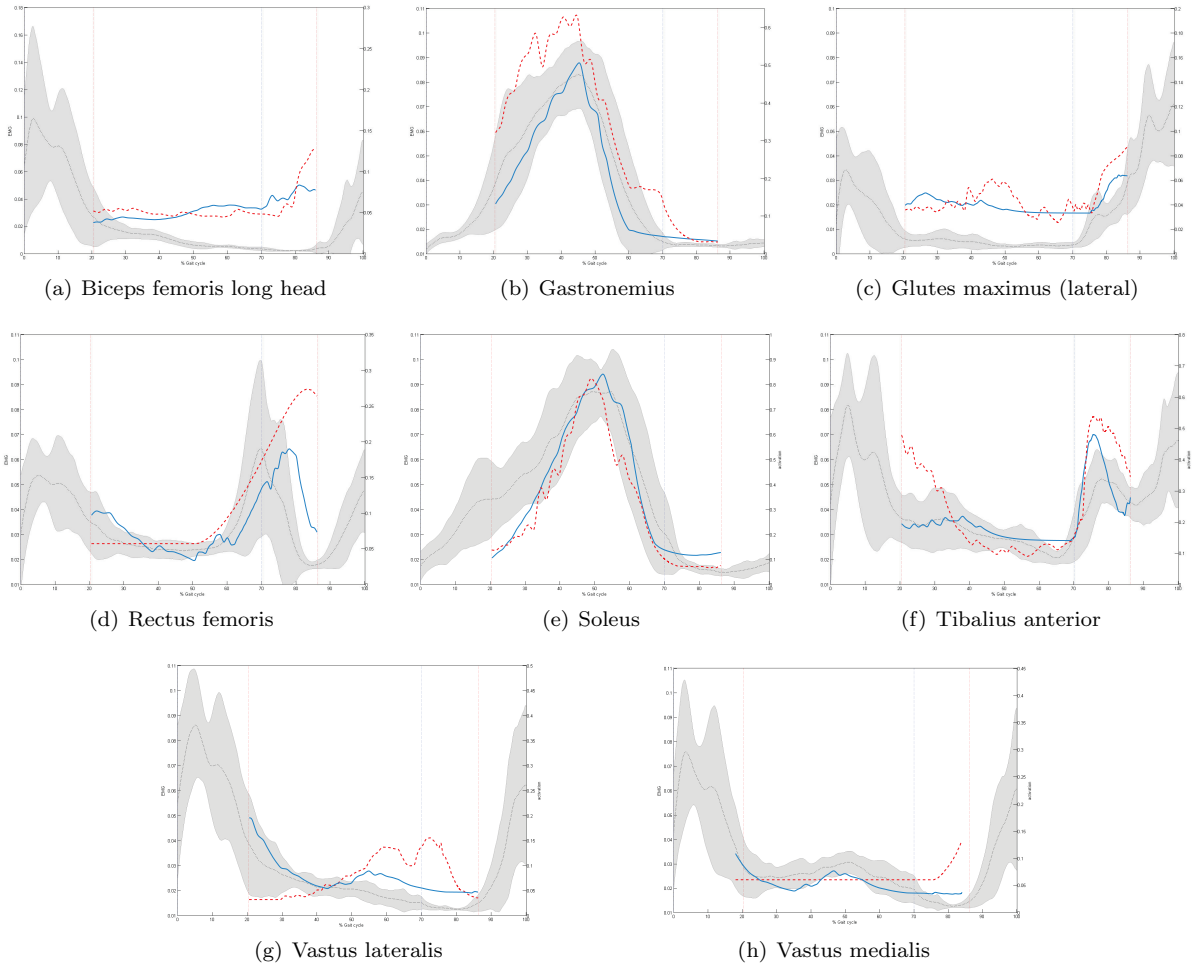

(a) Biceps femoris long head (b) Gastronemius (c) Glutes maximus (lateral)

(d) Rectus femoris (e) Soleus (f) Tibalius anterior

(g) Vastus lateralis (h) Vastus medialis

Fig. 6 Comparison of experimental and simulated muscle activity between the geometry knee joint (blue solid line) and the planar knee joint (red dashed line). The shaded area represents ±1 standard deviation of the EMG using 28 gait motions.

From the CMC result its clear that muscle spanning over the hip, knee and ankle joint are all affected by different knee joint descriptions.

3.3 Joint Reaction

To better understand the difference between the two knee models and there effect on hip and knee joint forces OpenSim were used to calculate the joint reaction using the muscle forces calculated during CMC (see section. 3.2)). In order to evaluate the calculated joint forces they were compared to data from OrthoLoad [5]. For the hip joint, five gait motions from four subjects (RHR, HSR, EBR and EBL) were extracted. The subjects were walking on a treadmill with a constant speed of 2 m/s. For the knee joint seven gait motions were downloaded from four subjects, (K1L, K3R, K4R and K5R). The subjects walked on a plan floor at the own speed. To process the data a full gait cycle were identified using the synchronized video sequence. The force data were then imported into MotionLab, normalized over the gait cycle and a standard deviation of ±1 were calculated for each joint and dimension. Joint reaction forces for the hip joint are shown in figure 7 alongside ±1 standard deviation of the in-vivo OrthoLoad forces. Forces calculated from joint reaction were normalized to %BW and moments to %BW*m.

In the superior hip joints direction (fig. 7(a)) both knee joint models show clear difference in force load. In the midstance phase, from 30% to 40% of the gait cycle, the planar knee joint model predict a decrease in superior force with a mean value of 62%BW compared to the geometry-based knee joint model. The second differences are between 55% to 70% of the gait cycle were the planar knee joint model show an increase in superior force with a mean value of 60%BW compared to the geometry-based knee joint model. Except these two phases both models predict similar forces in the superior hip joint direction as presented in the OrthoLoad

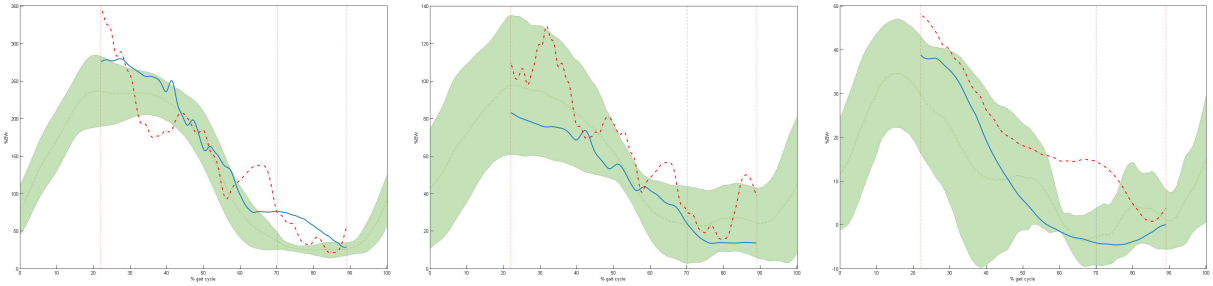

(a) Superior hip force (b) Lateral hip force (c) Anterior hip force

Fig. 7 Comparison of in-vivo measured hip joint forces and simulated joint reaction forces, geometry-based knee joint visualized as blue solid line, planar knee joint visualized as red dashed line. Green shaded area represents ±1 standard deviation of in-vivo measured hip forces from the OrthoLoad database.

data. In the lateral direction of the hip joint (fig. 7(b)) both the geometry-based knee joint model and the planar knee joint model display oscillations in the force estimation. This oscillation is more prominent in the planar knee joint model which also produced a higher force value with a mean difference of 19%BW. In the lateral direction of the hip join the geometry-based knee joint model display a better corresponding with the forces presented in OrthoLoad. For anterior forces in the hip joint the geometry-based knee joint model display the same trend and values as shown in the OrthoLoad data. The planar knee joint predict slightly higher values during the mid-stance phase. During toe-off (60% to 80% of the gait cycle) the planar knee joint estimate higher forces with a mean value of 8% BW.

In figure 8 knee joint reaction forces are shown from both models, including the ±1 standard deviation from Orthoload. Knee forces predicted in anterior (fig. 8(a)), lateral (fig. 8(c)) and superior (fig. 8(e)) direction of the knee joint show a clear trend between the two different joint models. In all three directions the planar knee joint model predicts higher forces then the geometry-based knee joint model. This is very clear in the anterior and lateral direction. In the lateral direction the planar knee joint model predicts higher forces both during the stance and swing phase (mean value of 70%BW). While in the anterior direction the largest differences occur between the two models during toe-off and the swing phase, with a mean difference of 13%BW. In the superior knee direction the planar knee joint model predict larger forces then the geometry-based knee joint model. During the stance phase the difference is %6.5 BW while during the swing phase the difference is 8% BW. An important detail in the anterior force is that the planar knee joint model predicts a double peak load (first before 22% and second at 40%) while the geometry-based knee joint only show a single load peak. In the OrthoLoad data an resemblance of a double peak load exist at 18% of the gait cycle, this comes from that only two of the four subjects have a double peak load. In superior direction the knee joint reaction data show two different results. During the stance phase the geometry-based knee joint model predict values close to OrthoLoads. During toe off the situation is the opposite, here the planar knee joint predicts a closer match to the OrthoLoad forces then the geometry-based knee joint model does. When it comes to moment forces in the the knee joint the lateral moment (fig. 8(d)) and superior (fig. 8(f)) moment display the same pattern. In both direction the planar knee predict a higher moment during both the stance and the swing phase. For the superior moment the planar knee joint show a higher mean value of 1.1%BW*m and in the lateral direction a higher mean value of 1.3%BW*m. In the lateral direction the geometry-base knee joint show the same pattern as the orthoLoad data, except during the swing phase were a higher value is predicted.In the superior direction no one of the knee joint show a good match to the OrthoLoad data. During the first part of the gait cycle the planar knee joint show a better prediction then the geometry-based knee joint. During the later part of the gait-cycle the geometry-based knee joint predict a closer match to the OrthoLoad data. In the knees anterior direction (fig. 8(b)) both the planar knee joint and the geometry-based knee joint predicted a smaller value than OrthoLoad . The anterior moment given by the geometry-based knee joint model resembles the pattern from OthoLoad data, the planar knee model show almost a constant value.

In general we can see that the planar knee joint produces higher loads in both the hip joint and the knee joint than the geometry-based knee joint model. The geometry-based knee joint model also predict forces closer too the forces present in the OrthoLoad data.

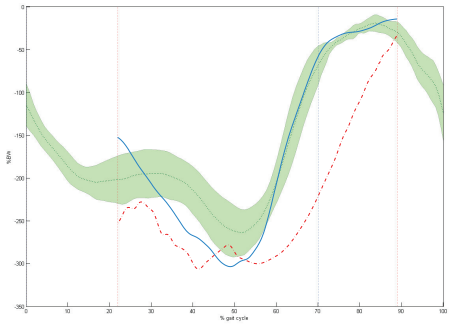

(a) Anterior knee forces

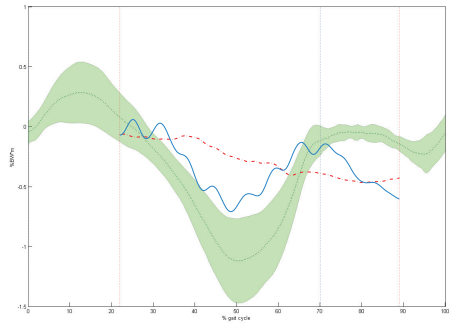

(b) Anterior knee moment

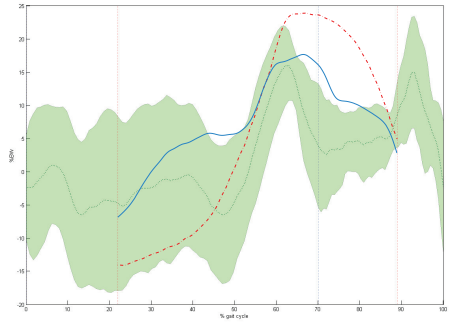

(c) Lateral knee force

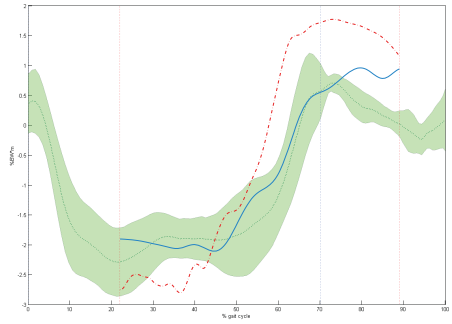

(d) Lateral knee moment

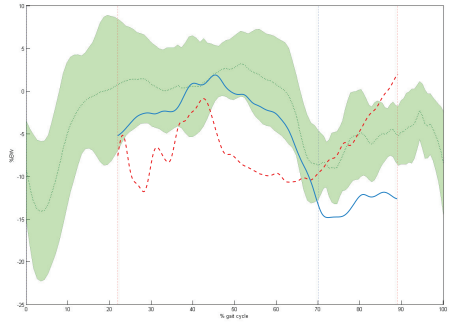

(e) Superior knee force

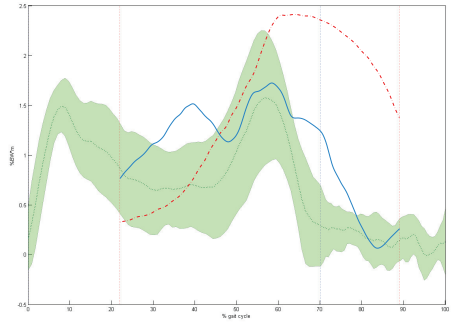

(f) Superior fig:cluster:kneeOrtho:superior:moment moment

Fig. 8 Comparison of in-vivo measured knee forces and simulated joint reaction forces, geometry-based knee joint visualized as blue solid line, planar knee joint visualized as red dashed line. The shaded area represents ±1 standard deviation of in-vivo measured knee forces from the OrthoLoad database.

4 Discussion

The use of neuromuscular models and simulations have given clinicians and researchers a tool to look deep into the functions of muscles, joints and bones and there effects on movability. Due to the complexity of these dynamic system we have to have absolute confidence in the accuracy of models and simulations before any decisions or conclusions are made. Most common when a new model is presented the results are validated against EMG. The use of surface EMG can provide some insight into a muscles behavior, but it can only validate a small set of muscles located close to the surface of the skin.

We believe that this is not enough when it come to validate new models or evaluate new joints dynamics. Therefore we believe that its absolutely necessary to evaluate using joint reaction forces which value incorporate all muscles spanning over a join. These joint reaction forces can then be compared to forces measured in-vivo, like data from the OrthoLoad project. The presented study constitute such a validation methodology, and providing further insight into the complexity of the human knee joint. To ensure an accurate kinematic solution great care were taken to minimize skin movements and other artifacts which can heavily effect inverse kinematic solutions. The two models used were

identical expect that in one model the geometry-based knee joint (see section. 2.1) were used and in the other the planar knee joint (see section. 4).

The first validation used in this study were inverse dynamics of the hip joint and the knee joint which were compared to literature data (fig. 4 and 5). The use of inverse dynamics provide a powerful tool to evaluate a model, but it does have some limitations. First inverse dynamics assumes that there is no friction inside the joint and that the mass distribution is uniformed in each segmented. Another prone error source are the misplacement of joint centers which alter the direction a body segment is accelerated. When solving the inverse dynamic problem an iterative process is used which starts from the ankle joint and propagate up in the model. Therefore errors that are introduced in the ankle joint solution propagate to the knee joint, which errors propagate to the hip joint and so forth. In the published inverse dynamic literature data large differences exist between the studies. For the knee joint *Kadaba et al., 1989* and *Cappozzo et al., 1975* predicts two different locations for the maximum knee flexion moment. The same literature data also predict two different patter fro the swing phase. For the hip joint uniform pattern are shown for adduction and rotation except small differences in value. For hip flexion large differences exist between the different studies, both in value and pattern. The inverse dynamic result presented using both models shows clearly that the knee joint description effects both the knee moment and the hip moment. All segments in both models were equal in lengths/weights and inertia matrixes. Therefore the differences inverse dynamic solutions can only come from the different kinematic each knee joints produced and differences in joint center.

To better evaluate the difference show in the inverse dynamic results computed muscular control were used to investigate both knee joints models and there effect on the model to produce the necessary muscle force needed to track the desired kinematics. The calculated muscle activation (fig. 6) corresponds with activation levels and patterns published in other gait studies [22]. For both knee joints the predicted activation agreed with the captured EMG, however for some muscles a clear difference existed. A common trend could be seen in the estimated muscle activations. For the geometry-based knee joint model lower muscle activation is needed to track the kinematic solution, then if the planar knee joint model is used. A larger difference can be seen in the GAS, RF and TA muscles that span all three joints in the lower limb. GAS and TA show large differences in activation during the mid-stance phase, while the RF shows a large difference during the swing phase. For VM, BFLH, VL and SOL only minor differences exist between the two knee models. To deeper investigate the difference between the knee models joint reaction forces were estimated (fig. 7, 8) and compared to forces available from the OrthoLoad database. However, the numbers of subject and motions available are too few to do any statistical analysis between the in-vivo forces and predicted model forces. Instead the ± 1 standard deviation calculated from OrthoLoad can only be used as an estimation of the in-vivo knee and hip joint forces. Both knee models predicted higher forces and moment then the OrthoLoad data showed. This overestimation of forces has been shown in other studies [17, 28] were result from neuromuscular models have been compared to in-vivo measurements. However some clear trends can be seen from this study. For the hip joint the geometry-based knee joint predict values that lies inside the ± 1 standard deviation while the planar knee joint predict much higher forces. This implies that forces predicted in the hip joint is highly dependent of the knee joint description. The same trend is present for both knee joints, the planar knee joint predicts larger knee forces in anterior, lateral and superior direction then the geometry-based knee joint or OrthoLoad in-vivo forces.

In this paper a new geometry-based knee joint model is presented and compared to in-vivo measurements. The result presented shows clearly that a geometry-based knee joint predict better muscle activation and joint reaction forces then a planar knee joint. However, this should be seen in the light of two limitations. Only one subject has so far been investigated and for this subject only one gait motion is included in this study. Investigations using more subjects and motions are currently performed.

5 Conflict of interest statement

None

Acknowledgements This work is supported by the European Marie Curie Program under the 3D ANATOMICAL HUMAN project (MRTN-CT-2006-035763). Motion capture were carried out at SMI, Aalborg University. MRI acquisition were carried out at UCL under supervision of Prof. Andrew Todd-Pokropek and Mitchelle Cheng.

References

1. Taka aki Moro-oka, Satoshi Hamai, Hiromasa Miura, Takeshi Shimoto, Hidehiko Higaki, Benjamin J. Fregly, Yukihide Iwamoto, and Scott A. Banks. Dynamic activity dependence of in vivo normal knee kinematics. *Journal of Orthopaedic Research*, 26(4):428–462, 2007.

2. S. Allaire, J.-J. Jacq, V. Burdin, and C. Roux. Ellipsoid-constrained robust fitting of quadrics with application to the 3d morphological characterization of articular surfaces. In *Engineering in Medicine and Biology Society, 2007. EMBS 2007. 29th Annual International Conference of the IEEE*, pages 5087 –5090, aug. 2007.
3. Frank C. Anderson and Marcus G. Pandy. Static and dynamic optimization solutions for gait are practically equivalent. *Journal of Biomechanics*, 34(2):153 – 161, 2001.
4. Edith Arnold, Samuel Ward, Richard Lieber, and Scott Delp. A model of the lower limb for analysis of human movement. *Annals of Biomedical Engineering*, 38:269–279, 2010. 10.1007/s10439-009-9852-5.
5. G Bergmann, G Deuretzbacher, M Heller, F Graichen, A Rohlmann, J Strauss, and G N Duda. Hip contact forces and gait patterns from routine activities. *J Biomech*, 34(7):859–71, Jul 2001.
6. Patrick Castagno, James Richards, Freenan Miller, and Nancy Lennon. Comparison of 3-dimensional lower extremity kinematics during walking gait using two different marker sets. *Gait & Posture*, 3(2):87 – 87, 1995.
7. Michael Damsgaard, John Rasmussen, Søren Tørholm Christensen, Egidijus Surma, and Mark de Zee. Analysis of musculoskeletal systems in the anybody modeling system. *Simulation Modelling Practice and Theory*, 14(8):1100 – 1111, 2006. SIMS 2004.
8. S.L. Delp, F.C. Anderson, A.S. Arnold, P. Loan, A. Habib, C.T. John, E. Guendelman, and D.G. Thelen. Opensim: Open-source software to create and analyze dynamic simulations of movement. *Biomedical Engineering, IEEE Transactions on*, 54(11):1940 –1950, nov. 2007.
9. S.L. Delp, J.P. Loan, M.G. Hoy, F.E. Zajac, E.L. Topp, and J.M. Rosen. An interactive graphics-based model of the lower extremity to study orthopaedic surgical procedures. *Biomedical Engineering, IEEE Transactions on*, 37(8):757 –767, aug. 1990.
10. Darryl D. DLima, Shantanu Patil, Nikolai Steklov, Shu Chien, and Clifford W. Colwell Jr. In vivo knee moments and shear after total knee arthroplasty. *Journal of Biomechanics*, 40(Supplement 1):S11 – S17, 2007. Interaction of Mechanics and Biology in Knee Joint Restoration and Regeneration.
11. Benjamin J. Ellis, Trevor J. Lujan, Michelle S. Dalton, and Jeffrey A. Weiss. Medial collateral ligament insertion site and contact forces in the acl-deficient knee. *Journal of Orthopaedic Research*, 24(4):800–810, 2006.
12. J. Fernandez and P. Hunter. An anatomically based patient-specific finite element model of patella articulation: towards a diagnostic tool. *Biomechanics and Modeling in Mechanobiology*, 4:20–38, 2005. 10.1007/s10237-005-0072-0.
13. U. Glitsch and W. Baumann. The three-dimensional determination of internal loads in the lower extremity. *Journal of Biomechanics*, 30(11-12):1123 – 1131, 1997.
14. F. De Groote, T. De Laet, I. Jonkers, and J. De Schutter. Kalman smoothing improves the estimation of joint kinematics and kinetics in marker-based human gait analysis. *Journal of Biomechanics*, 41(16):3390 – 3398, 2008.
15. Bernd Heinlein, Ines Kutzner, Friedmar Graichen, Alwina Bender, Antonius Rohlmann, Andreas M. Halder, Alexander Beier, and Georg Bergmann. Complete data of total knee replacement loading for level walking and stair climbing measured in vivo with a follow-up of 6-10 months. *Clinical Biomechanics*, 24(4):315 – 326, 2009.
16. Klein Horsman. *The Twente Lower Extermity Model*. PhD thesis, Department of Engineering Technology, University of Twente, Netherlands, 2007.
17. Morrison J.B. Function of the knee joint in various activites. *Biomedical Engineering*, 4:573–580, 1969.
18. M P Kadaba, H K Ramakrishnan, M E Wootten, J Gainey, G Gorton, and G V Cochran. Repeatability of kinematic, kinetic, and electromyographic data in normal adult gait. *J Orthop Res*, 7(6):849–60, 1989.
19. R. E. Kalman. A new approach to linear filtering and prediction problems. *Transactions of the ASME – Journal of Basic Engineering*, 82:35–45, 1960.
20. H. Kurosawa, P.S. Walker, S. Abe, A. Garg, and T. Hunter. Geometry and motion of the knee for implant and orthotic design. *Journal of Biomechanics*, 18(7):487 – 491, 493–499, 1985.
21. I. Kutzner, B. Heinlein, F. Graichen, A. Bender, A. Rohlmann, A. Halder, A. Beier, and G. Bergmann. Loading of the knee joint during activities of daily living measured in vivo in five subjects. *Journal of Biomechanics*, 43(11):2164 – 2173, 2010.
22. May Q. Liu, Frank C. Anderson, Michael H. Schwartz, and Scott L. Delp. Muscle contributions to support and progression over a range of walking speeds. *Journal of Biomechanics*, 41(15):3243 – 3252, 2008.
23. D. P. Pioletti, L. R. Rakotomanana, J. F. Benvenuti, and P. F. Leyvraz. Viscoelastic constitutive law in large deformations: application to human knee ligaments and tendons. *Journal of Biomechanics*, 31(8):753 – 757, 1998.
24. N.A. Ramaniraka, P. Saunier, O. Siegrist, and D.P. Pioletti. Biomechanical evaluation of intra-articular and extra-articular procedures in anterior cruciate ligament reconstruction: A finite element analysis. *Clinical Biomechanics*, 22(3):336 – 343, 2007.
25. Anders Sandholm, Nicolas Pronost, and Daniel Thalmann. Motionlab: A matlab toolbox for extracting and processing experimental motion capture data for neuromuscular simulations. In Nadia Magnenat-Thalmann, editor, *Modelling the Physiological Human*, volume 5903 of *Lecture Notes in Computer Science*, pages 110–124. Springer Berlin Heidelberg, 2009.
26. Jérôme Schmid and Nadia Magnenat-Thalmann. Mri bone segmentation using deformable models and shape priors. *Medical Image Computing and Computer Assisted Intervention*, pages 119–126, 2008.
27. Jerome Schmid, Anders Sandholm, Francois Chung, Daniel Thalmann, Herve Delingette, and Nadia Magnenat-Thalmann. Musculoskeletal simulation model generation from mri data sets and motion capture data. In Nadia Magnenat-Thalmann, Jian J. J. Zhang, and David D. D. Feng, editors, *Recent Advances in the 3D Physiological Human*, pages 3–19. Springer London, 2009.
28. W. R. Taylor, M. O. Heller, G. Bergmann, and G. N. Duda. Tibio-femoral loading during human gait and stair climbing. *Journal of Orthopaedic Research*, 22(3):625–632, 2004.
29. Darryl G Thelen and Frank C Anderson. Using computed muscle control to generate forward dynamic simulations of human walking from experimental data. *J Biomech*, 39(6):1107–15, 2006.
30. P.S. Walker, J.S. Rovick, and D.D. Robertson. The effects of knee brace hinge design and placement on joint mechanics. *Journal of Biomechanics*, 21(11):965 – 967, 969–974, 1988.
31. Jeffrey A. Weiss, Bradley N. Maker, and Sanjay Govindjee. Finite element implementation of incompressible, transversely isotropic hyperelasticity. *Computer Methods in Applied Mechanics and Engineering*, 135(1-2):107 – 128, 1996.
32. Gary T. Yamaguchi and Felix E. Zajac. A planar model of the knee joint to characterize the knee extensor mechanism. *Journal of Biomechanics*, 22(1):1 – 10, 1989.